Comprehensive Studies of Hydrogeophysical Potential of Groundwater Occurrences in Djohong Municipality, Adamawa Cameroon

Abdou Raouf
China University of Mining Technology: China University of Mining and Technology
NJEUDJANG KASI (kasinj2006@yahoo.fr)
University of Maroua: Universite de Maroua
Jianhua Yue
China University of Mining Technology: China University of Mining and Technology
Haiyan Yang
China University of Mining Technology: China University of Mining and Technology
Fengping Li
China University of Mining Technology: China University of Mining and Technology

Research Article

Keywords: Djohong municipality, VES, Aquifer, Ferruginous sediments, Metaconglomerates.

Posted Date: March 18th, 2022

DOI: https://doi.org/10.21203/rs.3.rs-1240286/v1

Abstract

Djohong municipality is located at the border between Eastern Cameroon and Central African Republic (CAR), in the Mbere division. The region is a shelter for thousands of people fleeing the socio-political crisis in CAR and it lacks safe drinking water supply. Surface water, rainwater, and shallow groundwater wells are the main water sources. As a result, deep aquifers appear to be an affordable solution to the widespread water demand gap in the region of Djohong. Forty-nine Schlumberger vertical electrical sounding (VES) were carried out in the framework of this study with maximum current electrode spacing of 240 m. The purpose was to investigate the occurrences of groundwater and related structural elements in the study area, which hosts two refugee camps, Ngam and Borgop. Eight geoelectric profiles were realized and their geological characteristics vary from the altered part to the bedrock, with ferruginous sediments and metaconglomerates in between. The altered part is composed of topsoil, travertines, sandy clay, clayey sand, and fractured shales with different geophysical characteristics. Two aquifer systems were highlighted, respectively in the altered soils of clayey sand and low permeability fractured rocks. The upper aquifer made of clayey sand is located in Ngam camp with thickness of 5 to 15 m and resistivity of 700 – 1500 Ω.m. The lower aquifer which is considered the main aquifer is located in both camps. It is hosted in the low permeability fractured shales of the Ngam camp, with resistivity of 200 to 1000 Ω.m and thickness of 34 to 82 m. In the Borgop camp, it occurs in the fractured granitic bedrock at about 8 and 19 m deep. Structurally, the study area is controlled by several potential faults, with NE – SW strike as a whole. The present study highlighted favourable conditions reducing geological and hydrogeological limitations to provision of safe drinking water for refugees of the two camps in Djohong.

1. Introduction

Daily internal and cross-border insecurity has exacerbated forced migration and uncoordinated displacement of populations. According to the latest report released by the United Nations High Commission for Refugees (UNHCR), there are about 80 million people displaced by war in the world today (ALJAZEERA 2020; UNHCR 2020). These people are sheltered in refugee camps while looking forward to return of peace in their homelands. Amnesty International (Basir and Aziz 2020) believes that this is the most serious global problem after the Second World War. Unfavourable living conditions at refugee camps marked with lack of basic needs of life such as drinking water, food and security has been exacerbated by Covid-19 pandemic (La Rosa et al., 2012, 2020; Meer and Mishra, 2021) and with significant impact on provision of drinking water (UN-Water 2010).

Since 2014, Djohong municipality has been recording a large number of refugees from the Central African Republic (CAR) (Sylvain and Cyrille 2017). They include a great diversity of ethnic groups (Arétouyap et al. 2017) and are seeking safe asylum (Aspinall and Watters 2010; Tazreiter 2010; De Abreu 2014). In Djohong Municipality, like all camps in the world, refugee settlements do not necessarily follow a clear pattern, and they settle in the cities/villages mainly according to their social status, ethnicity, or religion. Prior to any intervention by the host country or Humanitarian non-governmental organizations (NGOs), the well-off are usually dispersed in the local indigenous community and the poor are concentrated in one geographical area. Arétouyap et al. (2017) studied their living conditions in the Borgop camp, focusing on Water supply, sanitation and personal hygiene promotion (WASH). They found that a large number of people (576 people) use only one catchment and spend more than 30 minutes to two hours a day collecting less than 15 litres of water.

These figures are quite high compared to the recommended Sphere Minimum Standard (SMS) of about 250 people per catchment (Sphere Project 2004, 2011, 2018; Young and Harvey 2004). Therefore, additional efforts need to be made to address these problems. Previously, at the World Summit on Sustainable Development in Johannesburg in 2002, world leaders, having recognised the indispensable role of water, laid strong bases, with a clear timetable, for rapidly meeting the world's current and future water needs. These bases are a set of commitments that focus on groundwater to make it more accessible to all (UN-Water 2010). Groundwater is particularly important in Africa, especially in remote and heavily polluted areas, where urbanization is little structured and most of the population live in poverty (Katuva et al. 2020; Elemile et al. 2021). Groundwater resources are the most appropriate sources to which attention may be turned for responding to communities water needs as they can be detected in almost all environments, with little investment in treatment (Foster et al. 2000).

Exploring relevant conditions that may aid provision of safe water resources in such areas is essential to improve the living conditions and livelihood of communities. Therefore, the purpose of this study is to explore the subsurface layers and the structural elements affecting the study area through geophysical surveys in order to delineate the water-bearing formations for healthy water supply in Djohong municipality. In the long term, the results of this work could provide clean water to displaced refugees and communities in these areas through open wells and boreholes.

2. General Settings

2.1. Location

Djohong municipality (Fig. 1) is one of the three municipalities of the Mbere department, located in the Adamawa region of Cameroon. It lies between the longitudes 14° E and 15° E and the latitudes 6° 30' N and 7° 30' N, which extends over an area of about 2653 km².

2.2. Geological and tectonic setting

The basement is composed of Precambrian plutonic and metamorphic rocks. Gneisses, amphibolites, migmatites and granites are the main outcrops at the edge of the Adamawa region (Ganwa et al. 2008). The tectonic evolution of the area is characterized by metamorphism of Late Proterozoic plutonic and metamorphic basement rocks in granites and migmatites (Ngangom 1983). Topsoil, travertines, clays, sands, shales are the main lithologies in the boreholes (BH1 – BH7) covering the study area (Fig. 2).

The bedrock is composed of Precambrian granitized migmatites that have been affected by weathering and tectonic constraints for thousands of years, and are quite altered (Dumont 1987; Ngako et al. 1991). They rarely outcrop in this area. At the hydrogeological level, the soils are very thick and saturated at their base (Noutchogwe 2010). Shallow valleys cut off the tabular relief.

Noutchogwe (2004) proposed the tectonic evolution of the area, and its main sequence is as follows: Precambrian, Upper Cretaceous and Cenozoic from bottom to top. In Precambrian, the large fault zones were formed due to tectonic compression. It is very important and corresponds to the Pan-African orogenic cycle. This stage of fracturing prepared the weak zones of dislocation in Gondwana from Cretaceous. In the Upper Cretaceous, the Gondwana dislocation was associated with the formation of intracontinental basins (Benue and

Djerem in Cameroon, Doba, Bake-Birao and Bousso in Southern Chad and Northern Central African Republic) and led to the opening of the Atlantic Ocean as a result of the reactivation of Central African Shear Zone and related fault zones (N30E, N70E, N – S and E – W). These faults are believed to be the main channels of alkaline lava deposition (Le Maréchal and Vincent 1972; Temdjim et al. 2005; Déruelle et al. 2007; Nkouandou et al. 2008; Mbowou et al. 2010) in the Cenozoic Adamawa plateau.

Some researchers such as Djomani and Hermine (1994), Djomani et al. (1995) and Reusch et al. (2010) have conducted geophysical (gravity, seismic, magnetic and magnetotelluric) studies within a regional framework, with particular interest for deep structural correlation outside the crust and sometimes related to underground fluid circulation (Toteu et al. 2004; Njonfang et al. 2006; Njanko et al. 2006). Other local studies are related to the crustal structure, geothermal activity along the Cameroon Volcanic Line (CVL) and sedimentary thickness of the basin (Njeudjang et al. 2020a; b). Kande-Houétchak (2008) study around the Mbere tectonic trough shows that the resistivity of granito-gneissic basement is larger than 10,000 Ω·m. The resistivity of the trench sedimentary pile is less than 10,000 Ω·m; the thickness is between 1800 m and 2000 m. The thickness of the sandstones overlying the conglomerates is less than 360 m. The audio-magnetotelluric profiles show that the Moho lies between 25 km and 35 km, separating the high resistivity crust (greater than 300,000 Ω·m) and the conductive upper mantle with resistivity less than 300,000 Ω·m (Ludovic Houetchak et al. 2013).

The hydrographic network is dense and sub-parallel to dendritic (Olivry 1986), but polygonal and less dense on the plains, plateaus or flat-topped hills. Moreover, it offers a unique lithology during low-water periods. The large catchment areas of Djerem and Mbere and their numerous tributaries (rivers and streams) drain the Djerem and Mbere basins respectively.

The stratigraphy under the study area (Fig. 2) can be described as follows (Stafford et al. 2010): from bottom to top, it consists of Precambrian basement, Cretaceous sediments and Upper Tertiary to Pleistocene sediments. The lower Cretaceous sediments may belong to “Continental Intercalaire”. They are located on the Precambrian granito-gneissic basement. Metaconglomerates, ferruginous conglomerates, ferruginous sandstones, ferrocalcariferous siltstones and shales compose the Cretaceous sediments. Metaconglomerates are usually located near faults and tend to follow different dips and strike direction. Shales are considered being the lower aquifer in Ngam area. The Cretaceous sediments are also composed of lateritic sandstones, grey claystones and grey argilo-ferruginous sandstones. For example, in the Yarmbang area (Fig. 3), these deposits are known as Yarmbang sequence. Sands, clays, agglomerates, clayey sandstones and travertines, represent Tertiary to Quaternary sediments.

3. Methods

3.1. Data acquisition

Forty-nine vertical electrical sounding (VES) were carried out in this study. Due to the urgent need for water in the area, only data from two refugee camps (Ngam and Borgop camps) were used for geoelectric profiles. These field VES data were selected as representative of the study (Fig. 3).

This investigation involved the use of Schlumberger’s arrangement for collecting data from study locations distributed along eight geoelectric profiles (see Fig. 3). The current electrode spacing (AB) ranges from 3m to

240m with progressive increasing distance to examine the subsurface of the area. The “ABEM SAS 300B” Terrameter was used to collect the data. Some VES points were established near existing wells (BH5 and BH7) with known petrology and groundwater levels, useful a-priori information to correlate with the VES results.

3.2. Data processing

The field data were inverted and analysed in 1D and 2D using the IPI2WIN software (Bobachev et al. 2002) based on the inverse problem. The process starts with the inversion step then automatically reduces the number of layers to a minimum, and end by editing the field curve. The aim of the process is to fit the observed and calculated data for estimating the Root Mean Square (RMS). For this study, the RMS limit was set at 2%. The purpose of the inversion is first to explain quantitatively the primary resistivity data collected from the field, and then to analyse the horizontal and vertical distribution of the layers. Two main steps describe the quantitative interpretation. The first is the Generalized Cagniard graphs method (Koefoed 1960, 1965a, b; Orellana and Mooney 1966) using the curve-matching method. The second step uses the computer software (IPI2WIN 2000) also known as analytical interpretation (Mohamaden et al. 2016; El_Hameed et al. 2017). At the end of this process, the lithology (N), total thickness of layers (d), depth of the survey (Alt), thickness of each layer (h), as well as the resistivity values (ρ) of the corresponding layers were calculated and displayed (see Fig. 4). These parameters can then be used for petrographic identification, groundwater characterization, and estimation of aquifer transmissivity (Oke 2019). Finally, the modelling data were represented as geoelectric profiles.

4. Results

Figure 4 shows the correlation between the interpretation results of field VES data and the lithology of the available boreholes in the study area. The blue curve is the result of inversion data, and the red curve is the result of apparent resistivity field data. Table 1 presents the interpretation curves along the area, resulting in eight geoelectric profiles, namely, traverses **1** to **8**.

Table 1 Results of the interpreted vertical electrical soundings

VES No.	Resistivity of layers (Ohm.m)						Thickness of layers (m)					
	L1	L2	L3	L4	L5	L6	L1	L2	L3	L4	L5	L6
0	887.1	2474	1468	2415			0.8	4.1	37.8			
1	2333	7751	2124	497.2	45832		0.5	5.6	19.1	39.6		
2	6429	14461	4426	1275	481.3	86125	0.9	1.2	9.10	14.7	34.1	
3	4295	13234	4017	1060	388	7142	0.9	1.18	9.1	14.7	34.1	
4	2689	11966	3082	611.2	15237		0.90	1.60	10.1	81.6		
5	2189	7875	2152	1564	584.3	3307	0.9	1.18	9.13	14.7	34.1	
6	1592	12950	2103	494.3	150373		0.74	1.22	15	27.6		
7	5647	7822	2557	867.5			2.14	2.96	7.1			
8	4465	10916	3664	555.9	71928		1.02	1.71	9.2	49.4		
9	1818	23317	1827	359.6	55466		0.73	1	20.6	27.8		
10	2022	13838	3774	811.3	2025		0.8	1	10	52.7		
11	2454	22977	3721	982.1	2018		0.9	1.2	9.12	48.9		
12	3339	16514	4056	692.2	11414		0.71	0.64	11.1	66.6		
13	2400	20610	3560	566.3	58334		0.7	1	9.52	46.9		
14	2400	16307	3351	1009	233.2	47431	0.7	1.5	4.6	18.7	37	
15	1639	19759	4572	514.3	4420		0.92	0.71	8	51.8		
16	1354	10447	4321	1597	830.5		1.5	2	4.23	4.8		
17	1596	6527	1818	361.4	46549		0.9	3.94	21	34		
18	4020	6130	2962	621.3	17979		0.6	3.3	11	81.9		
19	2046	6350	928.6				0.44	7.23				
20	2999	13362	2516	602.2	44063		0.74	1.4	12	58.2		
21	3047	14448	3612	643.3	26513		0.88	1.6	11	77.8		
22	1910	7601	1452	378.6	86199		0.5	5.4	19.7	35.1		
23	2201	6545	898				0.5	9.35				
24	2606	9071	4808	862.3	437.8	2111	0.9	1.2	9.10	14.7	34.1	
25	6268	18584	6291	1786			0.9	1.2	9.10			
26	4357	8134	2908	791.5	1036		0.9	3.93	6.4	14.7		
27	1648	5000	498.1	5976			0.32	9.3	79.6			
28	1521	4861	506.1	12275			0.4	8.7	63.9			

29	8062	12046	2347	1086	103.3		0.9	3.3	15.3	22.2	
30	4149	2112	1948	27.86			1.1	19.3	7.2		
31	13756	6122	88.3				1.98	10.5			
32	345.8	926.5	3438	159.5			0.9	8.14	10.3		
33	343.6	493	1135	381.3			0.9	8.1	32.7		
34	1953	4800	1827	302	3902		0.9	1.2	9.1	49.2	
35	998.8	2035	206.4	50557			0.3	13.3	27.1		
36	1360	4238	2816	664.6	8826		0.9	1.5	10	55.4	
37	769	2830	62.04	1244			1	7.4	7.2		
38	831.9	9764	1735	551.7	12493		0.72	0.91	17	31.9	
39	407.7	896.3	239.5	1755			0.9	10.3	14.7		
40	296.8	9159	343.6				1.5	6.2			
41	292.1	7035	669.1	150.1	542.3		0.9	1.2	8.4	14.7	
42	880	2693	574.4	29260			0.9	10.3	48.8		
43	922.1	8321	1413	355.7	59759		0.81	1.23	10.9	38.5	
44	237.5	1210	282.3	850.3	15500		0.86	0.93	2.13	66.6	
45	470	732.6	254.6	1305	407.5	63244	0.9	1	2.23	15.4	22.2
46	130.7	310.6	54658				1.35	29			
47	3502	6131	2723	493.5			0.9	1	7		
48	8296	882.2	378.7	21916			1.55	14	17.1		

4.1. Apparent resistivity maps

Figure 5 shows from top to bottom the apparent resistivity slice maps in the study area with AB values of 3, 8.8, 26.4, 38, 55 and 116 m. The selection of AB values is based on the changes in resistivity values observed on the maps. These maps show lateral variations in resistivity in the depth range of 0.75 – 1, 2.20 – 2.93, 6.6 – 8.8, 9.5 – 12.66, 13.75 – 18.33 and 29 – 38.67, respectively.

The surficial apparent resistivity maps are characterized by high resistive units, with values as high as 9400 Ω·m (VES 0, 1, 2, 3, 7, 8, 9, 12, 13, 18, 20, 21, 25, 28, 34, 35, 36, 37, 38, 42, and 43) and low resistive units with values as low as 500 Ω·m, which indicate the heterogeneity of the formations in the study area.

From an apparent depth of 6.60 – 8.80 m downwards, low apparent resistivity areas become more important with increasing depth of investigation (DOI). The low resistivity units are characteristics of the aquifer in this area.

From the apparent depths of 9.5 – 12.66 m and 13.75 – 18.33 m downwards, the corresponding maps show almost similar resistivity values as if they were collected on the same geological layer. Furthermore, the resistivity values decrease slightly with increasing DOI, which may be due to the influence of water saturation.

The deepest apparent resistivity maps show an irregular distribution of resistivity values and the high resistivity values are higher compared with the shallower portions. However, they are better distributed at Borgop camp.

4.2. Geoelectrical cross-sections

Eight geoelectric profiles are selected to represent the area (Fig. 3), six of which are from Ngam camp (Fig. 6) and two from Borgop camp (Fig. 7). Moreover, Figures 6 and 7 also show the correlation between the geoelectric cross-sections (Traverse **1**, **6** and **8**) and the apparent resistivity cross-sections (with depth) in the study area. The purpose is to compare the existing geological structures and clearly infer faults. The processing and interpretation of all the data in the study area are described below.

4.2.1. Ngam camp

The first geoelectric unit is a thin layer of resistive material, which forms the topsoil with resistivity values of 1300 – 6500 Ω·m and thickness between 0.5 and 2 m. This resistivity range may correspond to the laterite (Arétouyap et al. 2015; Meying et al. 2018). In some VES, this layer may also be formed by dry sand. This layer occurs in all VES of Ngam (Fig. 6).

The second geoelectric unit is the travertines layer. It also consists of a mixture of topsoil and laterite. This heterogeneity results in large variations in resistivity values (6000 – 23000 Ω·m). Its thickness ranges from 1m to 6 m. This layer appears in all VES of Ngam.

The third geoelectric unit is sandy clay with resistivity between 1000 and 6200 Ω·m. Some VES in this layer may contain dry sand and limestone from travertines, which may explain its wide resistivity range. The thickness of this layer is between 6 m and 21 m. This layer exists in all VES of Ngam except VES 7 and 8 (Traverses **5** and **6**).

The fourth geoelectric unit is of clayey sand lens only detected in VES 2, 3, 5, 16 and 26 (Traverses **1**, **4**, **5**, and **6**) with low resistivity values (700 – 1500 Ω·m) and thickness ranging from 5 m to 15 m. This low resistivity layer is surrounded by high resistivity layers. This is a conductive area (also known as an anomaly). In addition, faults have been inferred in this layer. The conductive area may indicate the target of groundwater. It is the upper aquifer of the area and its depth ranges from 8 to 13 m.

The fifth geoelectric unit has resistivity values between 200 and 1000 Ω·m and thickness ranging from 34 m to 82 m. This layer is a conductive area formed of shales, some intercalation of thin sandstones lenses and highly fractured zones. The conductive area may suggest a target of groundwater. This layer is the lower aquifer of the area and occurs in all VES of Ngam except VES 25 (Traverses **1** and **3**) extending to the maximum depth of survey in VES 7, 16 and 26 (Traverses **1**, **5** and **6**). Its age is Cretaceous.

The sixth geoelectric unit has resistivity values between 1000 – 3000 Ω·m and may consist of ferruginous sediments lens composed of sandstones and conglomerates mixture. The thickness of this layer varies from 7 m to 11 m. It occurs in VES 7 and 8 (Traverses **5** and **6**), where an important telluric field has been noted during field measurements and may be of Cretaceous age.

The seventh geoelectric unit may compose of Cretaceous Metaconglomerates (Le Maréchal and Vincent 1972; Stafford et al. 2010) with resistivity values ranging from 1500 to 3000 Ω·m. This layer is only found in VES 5, 11, 24 and 25 (Traverses **1**, **3**, **4**, **5** and **6**). The upper surface of this layer appeared in the depths range of 10 m to 51 m, while the lower surface extends to the maximum depth of survey.

The eighth geoelectric unit is Precambrian in age and has resistivity values between 2000 – 150,000 Ω·m. It may consist of granite which constitutes the bedrock of the area. The upper surface of this layer appeared in the depths range of 45 m to 97 m, while the lower surface extends to the maximum depth of survey.

4.2.2. Borgop camp

The first geoelectric unit has resistivity values between 200 and 7000 Ω·m and thickness ranging from 0.6 m to 1.5 m. It is topsoil layer, which may have formed of laterite, clays, and sand and occurs in all VES of Borgop camp.

The second geoelectric unit is sandy clay with resistivity ranging from 600 to 9500 Ω·m. This wide range in resistivity values is due to the expected intercalation of clay and dry sand with limestone in some VES. Its thickness is between 1 m and 11 m and was detected in all VES of Borgop.

Located at VES 0, 36 and 38 with resistivity range of (600 – 1700) Ω·m and thickness varying from 10 to 38 m, the third geoelectric unit at Borgop camp is composed of coarse sand and fine gravels from tertiary to Quaternary. In some VES, this layer may consist of clay sand nodules and limestone, which may explain its wide resistivity range.

The fourth geoelectric unit is ferruginous sediments with thickness up to 11 m. This layer has a resistivity value up to 1400 Ω·m and characterized by an important telluric field around VES 43 (Traverse **7**). It may include gravels or pebbles, showing typical features of metaconglomerates and conglomerates.

The fifth geoelectric unit consists of Cretaceous Metaconglomerates with resistivity values between 500 and 2400 Ω·m and was found only in VES 0 and 41. This layer refers to the Metaconglomerates of Borgop stream, formerly known as “Borogounous conglomerates” (Bresson et al. 1952; Roch 1953), and to the Metaconglomerates of Bah stream and Ka-Borgop mountain (Le Maréchal and Vincent 1972). The upper surface of this layer appeared in the depths range of 24 m to 43 m, while the lower surface extends to the maximum depth of survey.

The sixth geoelectric unit is the granitic bedrock and is composed of two parts, namely, shallow part and deep part. The shallow part is fractured and appears conductive. It represents the upper aquifer of the area while the deep part is devoid of fractures and constitutes the bedrock with resistivity up to 59,000 Ω·m. The resistivity of the shallow part ranges from 60 to 500 Ω·m with thickness ranging from 7 to 49 m (VES 37, 38, 41, 42 and 43). In VES 40, the fractured part extends to the maximum depth of survey. The age of this unit is Precambrian.

4.3. Depth and true resistivity maps

VES data of Ngam and Borgop camp were used to study potential future drilling locations. To achieve this purpose, different maps were built (Figs. 8 – 11) using Kriging gridding method (Goovaerts 1998, 2001; Gorai et al. 2015): depth of the aquifers (upper and lower), depth of the lower aquifer, true resistivity of the aquifers (upper and lower), true resistivity of the lower aquifer, and thickness of the lower aquifer were established.

4.3.1. Ngam camp

Figures 8 and 10 show an increase of depth and thickness of the lower aquifer (fifth geoelectric unit) in the North-Eastern and Eastern parts, respectively, while the true resistivity values of the aquifers and lower aquifer (fifth unit) increase with the trend of NE – SW (Fig. 9). The general trend of these true resistivity values in NE – SW direction is consistent with the trend of hydrographic network and faults in the study area (Figs. 1 and 3).

4.3.2. Borgop camp

Figures 11 **(a)** and **(b)** show a decrease in aquifer depth and thickness in the Northeast and East, while they increase in the Southwest. Fig. 11**(c)** shows the decline of resistivity values in the trend of N–S, especially towards the East side. These low resistivity values are the characteristics of conductivity anomalies in this area, which may indicate the existence of groundwater.

5. Discussions

The analysis and interpretation of the geophysical results are helpful to identify different geoelectric layers. From top to bottom, the study area is composed of topsoil, travertines, sandy clay, clayey sand, fractured shales, ferruginous sediments, and metaconglomerates covering granitic bedrock. In addition, complex fault/fracture systems affect the study area making some layers appear in some VES but not in others. These inferred faults on the North and South sides control the flow and accumulation of groundwater in the area.

Geoelectric data processing reveals conductive anomaly areas of low resistivity, which could be interpreted as targets of groundwater. In Ngam camp these areas are highlighted in two geoelectric units (fourth unit and fifth unit), which form the upper and lower aquifers of the area respectively (Fig. 6). The upper aquifer is about 8 to 13 m deep; and the lower aquifer at about 12 to 27 m deep (Fig. 8b). Groundwater in this camp mainly occurs in the altered soils of clayey sand and low permeability fractured rocks such as shales (Fig. 6**)** with a large thickness (Fig. 10). Despite their low permeability, this aquifer could be exploited in this community (MacDonald and Davies 1998, 2019; MacDonald et al. 2001). However, due to the limited water resources of aquifers in this environment, special attention must be paid to the establishment and management of wells or boreholes, otherwise the possibility of success is very low (Davies and Dochartaigh 2002).

In Borgop camp, the conductive zones occur in shallow fractured bedrocks between 8 and 19 m deep (Fig. 11a). All these aquifers are similar to those obtained by Betah (1976), Djeuda Tchapnga (1987), Kana et al. (2015) and Meying et al. (2018) in Northern Cameroon, and Teikeu et al. (2012) in Yaoundé. Thus, these aquifers constitute the main aquifers in the area and are independent (Mafany et al. 2006). In addition, some geoelectric layers were also depicted in the altered soils, which are ferruginous sediments and metaconglomerates. Ferruginous sediments disrupt good data collection during field measurements through their important telluric field. This

characteristic may be attributed to their ferruginous cement (Stafford et al. 2010). According to Stafford et al. (2010), ferruginous sediments show typical features of metaconglomerates and initially unmetamorphosed. As for metaconglomerates, they appear discontinuously in the study area in some VES (0, 5, 11, 24, 25 and 41). This could be due to their location near faults and consequently follows different dips and strike directions (Stafford et al. 2010). Furthermore, their presence in the study area may relate to the Metaconglomerates of Borgop stream, formerly known as “Borogounous conglomerates” (Bresson et al. 1952; Roch 1953), and to the Metaconglomerates of Bah stream and Ka-Borgop mountain (Le Maréchal and Vincent 1972).

Interpretation of the apparent resistivity maps (Fig. 5) shows an irregular distribution of resistivity values in the area with a decrease in low-apparent resistivity values with depth. In fact, low apparent resistivity areas reflecting conducting anomaly could be associated with target of groundwater and high resistivity to the laterite and travertines. For instance, in surficial apparent resistivity maps (Fig. 5), low apparent resistivity areas are associated with the zones of interest for dry season agriculture while at the apparent depth of 6.60 – 8.80 m downwards; they may indicate the existence of aquifers or clay layers. Meanwhile, from the apparent depths of 9.5 – 12.66 m and 13.75 – 18.33 m downwards, these areas are well surrounded by high resistivity, which can be attributed to granitic bedrock. The corresponding low resistivity areas are conducive to groundwater research. This corroborates the findings of Mbog et al. (2019) in the Douala sedimentary basin.

The analysis of true resistivity maps and depth maps of the study area (Figs. 8 – 11) allows mapping low and high resistivity contours and depths, which could be useful for determination of future location areas for new wells in the study area. In fact, the definition of such areas must obey the following criteria: first, select areas with large aquifer thickness and moderate depth. This is to avoid or reduce any potential groundwater contamination or pollutants (Mafany et al. 2006; Ako et al. 2014; Li et al. 2018; Koelmans et al. 2019; Akenji and Tarkang 2019; Mintenig et al. 2019; Sako et al. 2020; Tantoh and McKay 2020; Genter et al. 2021). Second, select highly fractured zones to avoid possible wells dehydration during the dry season. This may be related to the migration of water to deep fractures in the same seasons. Therefore, in Ngam camp, the future location areas follow NE – SW trend, while in Borgop camp, their direction is N – S, more specifically the east side. Moreover, the two orientations (NE – SW and N – S) are consistent with the flow trend of hydrographic network (such as Mbere and streams) and faults in the study area (Figs. 1 and 3). In other words, the groundwater in the study area is likely to flow to the Mbere River and its streams, which constitute the main drainage axes of the area.

6. Conclusion

Forty-nine vertical electrical soundings were conducted to provide information on the subsurface layers and associated structural elements beneath the study area. The apparent resistivity maps (Fig. 5) revealed that the study area has both high and low resistivity values, which can be attributed to the heterogeneous formations in the area. The areas of low apparent resistivity can be used for dry season agriculture while the areas of high resistivity are characteristic of either surface laterites or travertines, or underlying granitic basement. In addition, an irregular distribution of resistivity values has been observed on the deepest maps with a particular increase in high resistivity values compared to the shallower portions. This irregularity may indicate that the study area is controlled by various structural elements. Geoelectric data processing reveals that in addition to structural elements, the study area is also composed of topsoil, travertines, sandy clay, clayey sand, fractured shales, ferruginous sediments, and metaconglomerates covering the granitic bedrock from top to bottom. Furthermore, two aquifer systems have been identified in the altered soils and low permeability fractured rocks forming upper

and lower aquifers respectively. These are respectively clayey sand and fractured shales in Ngam camp and fractured granitic bedrock in Borgop camp. In Ngam camp, the depth of clayey sand is about 8 to 13 m and the fractured shales is about 12 to 27 m, while in Borgop camp, the fractured granitic basement is between 8 and 19 m deep. Structurally, the study area is affected by several probable faults, the general trend of which is NE – SW. Although the permeability of these aquifers are very low, given the current demographics of the area and other reported geological and hydrogeological conditions, they can be exploited as water sources for mitigation of worsening water needs at the refugee camps. With special attention on establishment and continuous management of wells or boreholes, sustainable water supply to the larger surrounding communities can be achieved.

Declarations

Compliance with ethical standards

The authors declare that they have no known competing financial interests or personal relationships that could have appeared to influence the work reported in this paper.

Acknowledgements

This paper is a part of the first author's PhD Dissertation at China University of mining and technology (Xuzhou, China). The authors would like to thankand appreciate Dr.Nicolò Giordano (Géotherma solutions Inc.)and Prof. Hermann Zeyen(Department of Earth Sciences, GEOPS Laboratory, Paris-Sarclay University, Paris-Sud University, CNRS, Orsay, France) for their constructive and thoughtful comments.

Funding

The Chinese Scholarship Council (Grant No. **2017DFJ014249**) supported this work.

References

1. Akenji N, Tarkang C(2019) A Quantitative Analysis of Anthropogenic Pollution on Ground Water in Douala. Acta Sci. Microbiol. 2:104–110. https://doi.org/10.31080/ASMI.2019.02.0438
2. Ako AA, Eyong GET, Shimada J, Koike K, Hosono T, Ichiyanagi K, Richard A, Tandia BK, Nkeng GE, Roger NN (2014) Nitrate contamination of groundwater in two areas of the Cameroon Volcanic Line (Banana Plain and Mount Cameroon area). Appl. Water Sci. 4:99–113. https://doi.org/10.1007/s13201-013-0134-x
3. ALJAZEERA(2020) Number of displaced people globally tops 80 million in 2020: UN [WWW Document]. URL https://www.aljazeera.com/news/2020/12/9/more-than-80-million-people-displaced-a-bleak-milestone-un. Accessed 27 September 2021
4. Arétouyap Z, Robert N, Philippe N, Jamal A (2015)Aquifers productivity in the Pan-African context. J. Earth Syst. Sci. 124:527–539
5. Arétouyap Z, Liku EO, Nka LB, Bagnem JE, ZamboEA(2017) Water and Hygiene Quality in the Borgop-Cameroon Refugee Camp and its Potential Adverse Impacts on Environment and Public Health. J. Environ. Sci. Public Health 1:139–150

6. Aspinall PJ, Watters C(2010) Refugees and asylum seekers: a review from an equality and human rights perspective. Research Report 52. Equality and Human Rights Commission.
7. Basir SM, Aziz SN(2020)Refugee Issues in the 21st Century: Challenges to Humanity and World Diplomacy. Jurnal Undang-Undang Dan Masyarakat, 25(0):53–58
8. Betah SS(1976)Complément sur la monographe nationale de l'eau (aspects eaux souterrraines).
9. Bobachev C(2002) IPI2WIN: A windows software for an automatic interpretation of resistivity sounding data. Moscow State University, 320
10. Bresson Y, Guiraudie C, Roch E (1952) Le fossé tectonique de la Mbéré (Nord Cameroun). Comptes Rendus Académie Sci. 234:640–641
11. Davies JO, Dochartaigh BE(2002)*Low permeability rocks in sub-Saharan Africa: groundwater development in the Tabora Region, Tanzania*.Nottingham, UK, British Geological Survey, 76pp. (CR/02/191N)
12. De Abreu CAS(2014)Human Security in Refugee Movements: The Case of Southern Africa (PhD Thesis). Tesis de doctorado). Tohoku University. Tohoku, Japan
13. Déruelle B, Ngounouno I, Demaiffe D(2007)The 'Cameroon Hot Line' (CHL): A unique example of active alkaline intraplate structure in both oceanic and continental lithospheres. Comptes Rendus Géosciences, 339(9):589–600
14. Djeuda Tchapnga HB(1987) Géologie et hydrologie d'un secteur de la zone mobile d'Afrique Centrale: région de Poli, Nord-Cameroun
15. Djomani P, Hermine Y(1994) Apport de la gravimétrie à l'étude de la lithosphère continentale et implications géodynamiques : étude d'un bombement intraplaque : le massif de l'Adamaoua (Cameroun)
16. Djomani YHP, Nnange JM, Diament M, Ebinger CJ, Fairhead JD(1995)Effective elastic thickness and crustal thickness variations in west central Africa inferred from gravity data. J. Geophys. Res. Solid Earth 100:22047–22070. https://doi.org/10.1029/95JB01149
17. Dumont JF(1987)Etude structurale des bordures nord et sud du plateau de l'Adamaoua : influence du contexte atlantique. Géodynamique 2:55–68
18. El_Hameed AG, El-Shayeb HM, El-Araby NA, Hegab MG(2017)Integrated geoelectrical and hydrogeological studies on Wadi Qena, Egypt. NRIAG J. Astron. Geophys. 6:218–229. https://doi.org/10.1016/j.nrjag.2017.03.003
19. Elemile OO, Ibitogbe EM, Folorunso OP, Ejiboye PO, Adewumi JR(2021) Principal component analysis of groundwater sources pollution in Omu-Aran Community, Nigeria. Environ. Earth Sci. 80, 690. https://doi.org/10.1007/s12665-021-09975-y
20. Foster S, Chilton J, Moencg M, Cardy F, Schiffler M(2000) Groundwater in rural development. The World Bank. https://doi.org/10.1596/0-8213-4703-9
21. Ganwa AA, Frisch W, Siebel W, Ekodeck GE, Shang CK, Ngako V(2008) Archean inheritances in the pyroxene–amphibole-bearing gneiss of the Méiganga area (Central North Cameroon): Geochemical and 207Pb/206Pb age imprints. Comptes Rendus Geosci. 340:211–222
22. GenterF, Willetts J, Foster T(2021) Faecal contamination of groundwater self-supply in low- and middle income countries: Systematic review and meta-analysis. Water Research, 117350. https://doi.org/10.1016/j.watres.2021.117350

23. Goovaerts P(1998) Geostatistics for Natural Resources Evaluation. Applied Geostatistics Series 483 pp. New York, Oxford: Oxford University Press. ISBN 0 19 511538 4. Geol. Mag. 135:819–842. https://doi.org/10.1017/S0016756898631502
24. Goovaerts P(2001) Geostatistical modelling of uncertainty in soil science. Geoderma, Estimating uncertainty in soil models 103:3–26. https://doi.org/10.1016/S0016-7061 (01)00067-2
25. Gorai A, Jain K, Shaw N, Tuluri F, Tchounwou P(2015) Kriging Analysis for Spatio-temporal Variations of Ground Level Ozone Concentration. Asian J. Atmospheric Environ. 9:247–258. https://doi.org/10.5572/ajae.2015.9.4.247
26. IPI2WIN(2000) IPI2WIN-1D Program: Programs set for 1-D VES data interpretation. Russia: Dept. of Geophysics, Geological Faculty, Moscow University
27. Kana JD, Djongyang N, Raïdandi D, Njandjock Nouck P, Nouayou R, Tabod TC, Sanda O(2015) Geophysical investigation of low enthalpy geothermal potential and ground water reservoirs in the Sudano-Sahelian region of Cameroon. J. Afr. Earth Sci. 110:81–91. https://doi.org/10.1016/j.jafrearsci.2015.06.007
28. Kande-Houétchak L(2008)Étude géophysique de la structure de la croûte le long du fossé tectonique de la Mbéré (Sud-Cameroun) (Doctoral dissertation, Thèse de Doctorat/Ph. D., Université de Yaoundé I)
29. Katuva J, Hope R, FosterT, Koehler J, Thomson P(2020) Groundwater and welfare: A conceptual framework applied to coastal Kenya. Groundwater for Sustainable Development, 10, 100314. https://doi.org/10.1016/j.gsd.2019.100314
30. Koefoed O(1960) A Generalized Cagniard Graph for the Interpretation of Geoelectrical Sounding Data. Geophysical Prospecting, 8(3):459–469. https://doi.org/10.1111/j.1365-2478.1960.tb01728.x
31. Koefoed O(1965a) A Semi-Direct Method of Interpreting Resistivity Observations*. Geophysical Prospecting, 13(2):259–282. https://doi.org/10.1111/j.1365-2478.1965.tb01934.x
32. Koefoed O(1965b) Direct Methods of Interpreting Resistivity Observations*. Geophysical Prospecting, 13(4):568–591. https://doi.org/10.1111/j.1365-2478.1965.tb01950.x
33. Koelmans AA, Mohamed Nor NH, Hermsen E, Kooi M, Mintenig SM, De France J(2019) Microplastics in freshwaters and drinking water: Critical review and assessment of data quality. Water Research, 155:410–422. https://doi.org/10.1016/j.watres.2019.02.054
34. La Rosa G, Fratini M, della Libera S, Iaconelli M, Muscillo M(2012)Emerging and potentially emerging viruses in water environments. Annali Dell'Istituto Superiore Di Sanità, 48(4):397–406. https://doi.org/10.4415/ANN_12_04_07
35. La Rosa G, Bonadonna L, Lucentini L, Kenmoe S, Suffredini E(2020) Coronavirus in water environments: Occurrence, persistence and concentration methods - A scoping review. Water Research, 179, 115899. https://doi.org/10.1016/j.watres.2020.115899
36. Le Maréchal A, Vincent PM(1972)Le Fossé crétacé du Sud-Adamaoua, Cameroun (Centre IRD de Bondy). 229–249. http://www.documentation.ird.fr/hor/fdi:17880
37. Le Maréchal A(1976) Géologie et géochimie des sources thermominérales du Cameroun : Thèse Univ. Paris VI, le 6 mars 1974 (Résumé de thèse). Cah. ORSTOMSérie Géologie 8:107–108
38. Li J, Liu H, Paul Chen J(2018)Microplastics in freshwater systems: A review on occurrence, environmental effects, and methods for microplastics detection. Water Research, 137:362–374. https://doi.org/10.1016/j.watres.2017.12.056

39. Ludovic Houetchak K, Joseph K, Jean Marie T, Robert N(2013)Geoelectric Structure of the Crust along the Mbere Trough (South Adamawa) from Audio-Magnetotelluric Data. Int. J. Geosci. 2013. https://doi.org/10.4236/ijg.2013.48115
40. MacDonaldAM, Davies J(1998)Groundwater development maps of Oju and Obi Local areas, eastern Nigeria [Publication - Report]. British Geological Survey. http://nora.nerc.ac.uk/id/eprint/500112/
41. MacDonald AM, Davies J, Peart RJ(2001) Geophysical methods for locating groundwater in low permeability sedimentary rocks: examples from southeast Nigeria. J. Afr. Earth Sci. 32:115–131. https://doi.org/10.1016/S0899-5362 (01)90022-3
42. MacDonald AM, Davies J(2019) Fractures in shale: the significance of igneous intrusions for groundwater flow. Geol. Soc. Lond. Spec. Publ. 479:71–79. https://doi.org/10.1144/SP479.10
43. Mafany GT, Fantong WY, Nkeng GE(2006) Groundwater quality in Cameroon and its vulnerability to pollution, in: Groundwater Pollution in Africa. CRC Press
44. Mbog MB, Kenfack JV, Ngon GF, Tassongwa B, Bayiga EC, Etame J(2019) Morpho-Structural Mapping Constraints from Geophysical and Test Pit Investigations: Case Study of the Bomkoul Locality in Douala Sedimentary Basin, Cameroon, Central Africa. Journal of Geoscience and Environment Protection, 7(10):136-153. https://doi.org/10.4236/gep.2019.710011
45. Mbowou GIB, Ngounouno I, Deruelle B(2010) Pétrologie du volcanisme bimodal du Djinga Tadorgal (Adamaoua, Cameroun) [WWW Document]. URL https://www.memoireonline.com/11/11/4948/Petrologie-du-volcanisme-bimodal-du-Djinga-Tadorgal-Adamaoua-Cameroun.html. Accessed 15 May 2021
46. Meer MS, Mishra AK(2021) GIS approach for mapping novel coronavirus in northern state of India, Jammu and Kashmir. Environ. Earth Sci. 80, 540. https://doi.org/10.1007/s12665-021-09856-4
47. Meying A, Wassouo Elvis BW, Daniel G, Théophile NM, Kelian K, Daniel NJ(2018) Hydrogeophysical Investigation for Groundwater Resources from Electrical Resistivity Tomography and Self-Potential Data in the Méiganga Area, Adamawa, Cameroon. Int. J. Geophys. 2018:1–14. https://doi.org/10.1155/2018/2697585
48. Mintenig SM, Löder MGJ, Prime S, Gerdts G(2019) Low numbers of microplastics detected in drinking water from ground water sources. Science of the Total Environment, 648:631–635. https://doi.org/10.1016/j.scitotenv.2018.08.178
49. Mohamaden MI, Hamouda AZ, Mansour S(2016) Application of electrical resistivity method for groundwater exploration at the Moghra area, Western Desert, Egypt. Egypt. J. Aquat. Res. 42:261–268. https://doi.org/10.1016/j.ejar.2016.06.002
50. Ngako V, Jegouzo P, Nzenti JP(1991)Le Cisaillement Centre Camerounais. Rôle structural et géodynamique dans l'orogenèse panafricaine. Compte Rendu de l'Académie des Sciences, Paris 315:457-463
51. Ngangom E(1983) Etude tectonique du fossé crétacé de la Mbéré et du Djerem, Sud-Adamaoua, Cameroun. Bull. Cent. Rech. Explor. - Prod. Elf-Aquitaine 7:339–347
52. Njanko T, Nédélec A, Affaton P(2006)Synkinematic high-K calc-alkaline plutons associated with the Pan-African Central Cameroon shear zone (W-Tibati area): petrology and geodynamic significance. J. Afr. Earth Sci. 44:494–510. https://doi.org/10.1016/j.jafrearsci.2005.11.016
53. Njeudjang K, Abate Essi JM, Domra JK, Teikeu WA, Njandjock Nouck P, Djongyang N, Tchinda R(2020a) Gravity investigation of the Cameroon Volcanic Line in Adamawa region: Geothermal features and structural

control. J. Afr. Earth Sci. 165:103809. https://doi.org/10.1016/j.jafrearsci.2020.103809

54. Njeudjang K, Domra JK, Tom A, Abate Essi JM, Djongyang N, Tchinda R(2020b) Curie point depth and heat flow deduced from spectral analysis of magnetic data over Adamawa volcanic region (Northern Cameroon): geothermal implications. SN Appl. Sci. 2(8):1330. https://doi.org/10.1007/s42452-020-3099-z
55. Njonfang E, Ngako V, Kwekam M, Affaton P(2006)Les orthogneiss calco-alcalins de Foumban–Bankim: témoins d'une zone interne de marge active panafricaine en cisaillement. Comptes Rendus Geosci. 338:606–616
56. Nkouandou OF, Ngounouno I, Déruelle B, Ohnenstetter D, Montigny R, Demaiffe D(2008)Petrology of the Mio-Pliocene volcanism to the North and East of Ngaoundéré (Adamawa, Cameroon). Comptes Rendus Geosci. 340(1):28–37. https://doi.org/10.1016/j.crte.2007.10.012
57. Noutchogwe TC(2004) Investigations géophysiques en bordure du plateau de l'Adamaoua (Cameroun): rapport de la gravimétrie à l'étude de la croûte terrestre (PhD Thesis). Thèse 3ème cycles, Université Yaoundé 1, Cameroun
58. Noutchogwe TC(2010) Investigation géophysique dans la région de l'Adamaoua par les méthodes gravimétriques et magnétiques: implications structurales et hydrogéologiques. Yaounde Univ. Yaoundé I
59. Oke SA (2019) Hydrogeophysical Appraisals for Surficial Aquifer Potentials of Sedimentary Basin of SW Nigeria. J. Eng. Appl. Sci. 14:3575–3582. https://doi.org/10.36478/jeasci.2019.3575.3582
60. Olivry JC(1986) Fleuves et rivières du Cameroun. Monogr. Hydrol. ORSTOM
61. Orellana E,Mooney HM(1966)Master table and curves for vertical electrical sounding data,3(8):459–469
62. Reusch AM, Nyblade AA, Wiens DA, Shore PJ, Ateba B, Tabod CT, Nnange JM(2010) Upper mantle structure beneath Cameroon from body wave tomography and the origin of the Cameroon Volcanic Line. Geochem. Geophys. Geosystems 11. https://doi.org/10.1029/2010GC003200
63. Roch E(1953) Itinéraires géologiques dans le Nord du Cameroun et le Sud-Ouest du Territoire du Tchad. avec la collab., pour la partie pétrographique, de... Impr. nationale
64. Sako A, Sawadogo S, Nimi M, Ouédraogo M(2020) Hydrogeochemical and pollution characterization of a shallow glauconitic sandstone aquifer in a peri-urban setting of Bobo-Dioulasso, southwestern Burkina Faso. Environ. Earth Sci. 79, 296. https://doi.org/10.1007/s12665-020-09041-z
65. Sphere Project (Ed.)(2004)Humanitarian charter and minimum standards in disaster response (2004 ed.), Oxfam Publ.
66. Sphere Project(2011)Humanitarian Charter and Minimum Standards in Humanitarian Response: The Sphere Handbook. The Sphere Project. https://doi.org/10.3362/9781908176202
67. Sphere Project (Ed.)(2018)the sphere handbook: Humanitarian charter and minimum standards in humanitarian response (Fourth edition). Sphere Association
68. Stafford TM, Ricard NNP, Salah MM, Said DA, Emmanuel EG(2010) Existence of late continental deposits in the Mbere and Djerem sedimentary basins (North Cameroon): Palynologic and stratigraphic evidence. J. Geol. Min. Res. 2:159–169. https://doi.org/10.5897/JGMR.9000024
69. Sylvain AD, Cyrille NJ(2017)Influx of Refugees and Transformations of Land Use: Case of the Borgop Land (Adamawa-Cameroon) 6. https://doi.org/DOI: 10.21275/ART20175652
70. Tantoh HB, McKay TJ(2020) Rural self-empowerment: the case of small water supply management in Northwest, Cameroon. GeoJournal 85:159–171. https://doi.org/10.1007/s10708-018-9952-6

71. Tazreiter C(2010) Local to Global Activism: The Movement to Protect the Rights of Refugees and Asylum Seekers. Soc. Mov. Stud. 9:201–214. https://doi.org/10.1080/14742831003603349
72. Teikeu W, Ndougsa Mbarga T, Njandjock NP, Tabod C(2012) Geoelectric Investigation for Groundwater Exploration in Yaoundé Area, Cameroon. Int. J. Geosci. 3:640–649
73. Temdjim R, Tchouankoue JP, Kamgang P, Tchoua F (2005) Sur l'existence d'un maar trachytique dans la ligne volcanique du Cameroun: le maar Mbalang-Djalingo dans la région de Ngaoundéré (Plateau de l'Adamaoua). Rev. Géographie Cameroun 17–18:67–72
74. Toteu SF, Penaye J, Djomani Y(2004)Geodynamic evolution of the Pan-African Belt in Central Africa with special reference to Cameroon. Can. J. Earth Sci. 41:73–85. https://doi.org/10.1139/e03-079
75. UNHCR(2020) Forced displacement passes 80 million by mid-2020 as COVID-19 tests refugee protection globally [WWW Document]. UNHCR. URL https://www.unhcr.org/news/press/2020/12/5fcf94a04/forced-displacement-passes-80-million-mid-2020-covid-19-tests-refugee-protection.html. Accessed 27 September 2021
76. UN-Water(2010) juillet. OMS | L'eau potable et l'assainissement reconnus comme un droit fondamental.https://www.who.int/water_sanitation_health/recognition_safe_clean_water/fr/
77. Young H, Harvey P(2004) The Sphere Project: The Humanitarian Charter and Minimum Standards in Disaster Response: Introduction. Disasters, 28:99. https://doi.org/10.1111/j.0361-3666.2004.00245.x

Figures

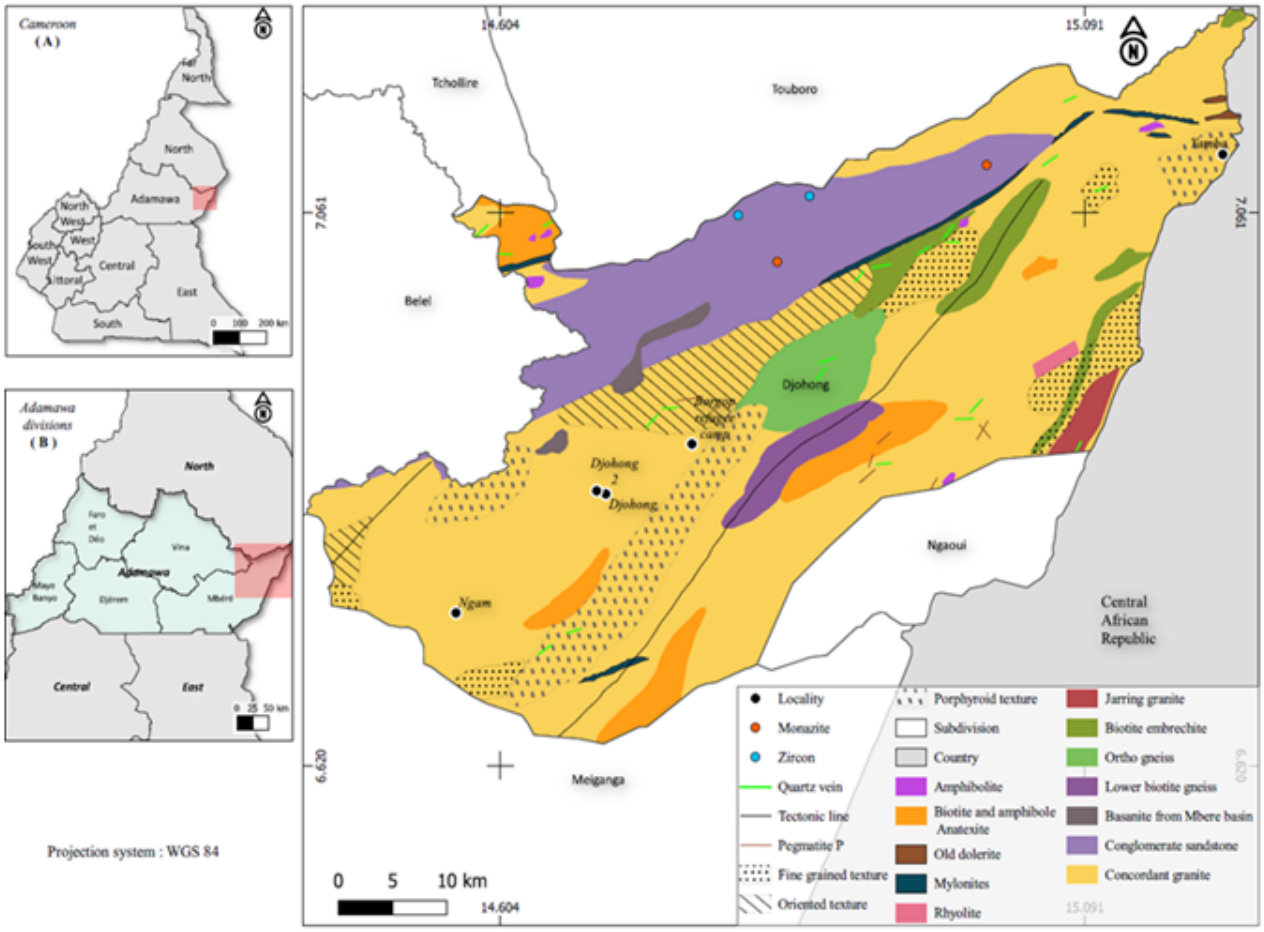

Figure 1

Geological map of the locality of Djohong (modified from the Adamawa map Le Maréchal, 1976).

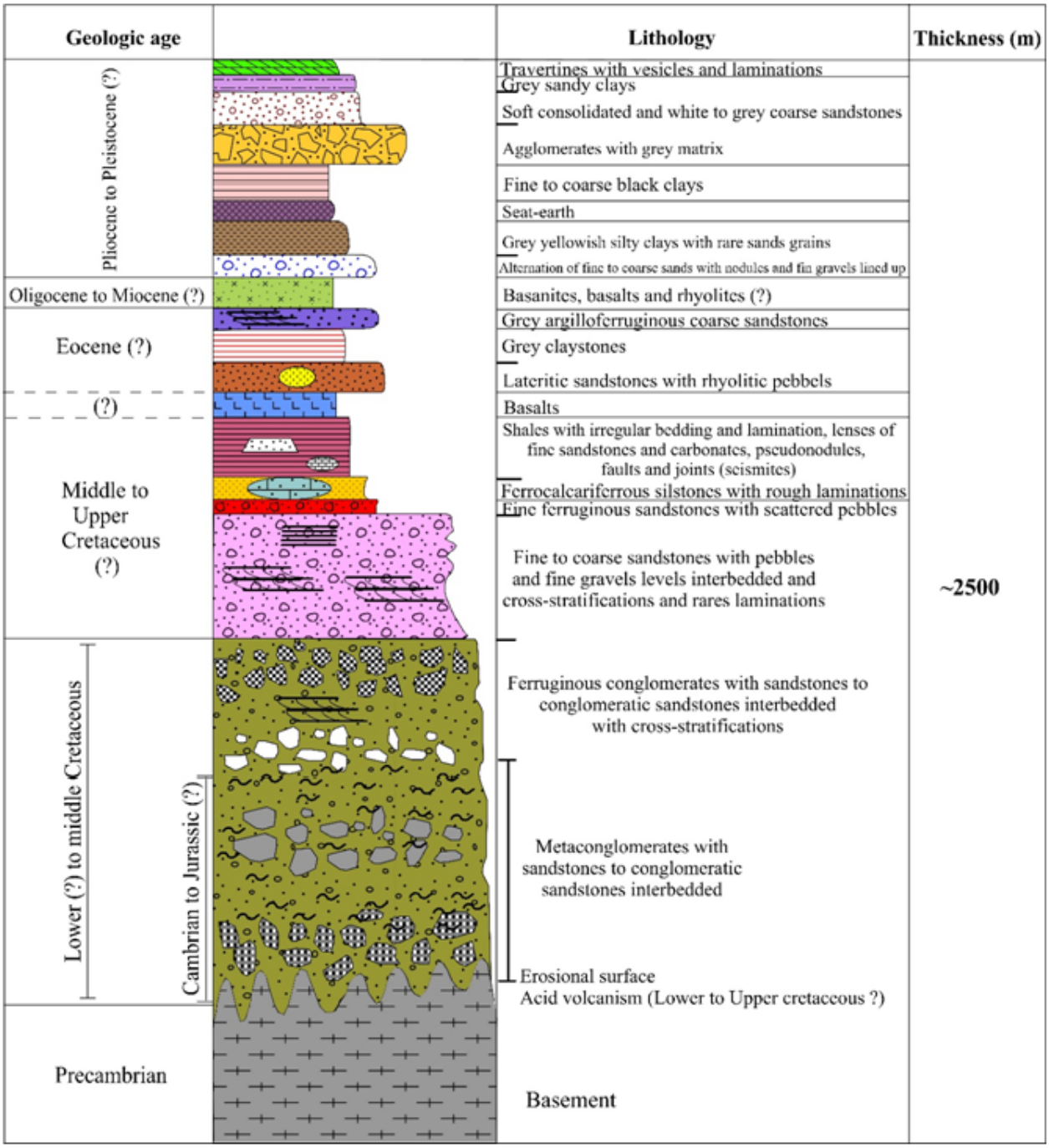

Figure 2

Stratigraphic column of the Mbere – Djerem basin (modified from Stafford et al., 2010).

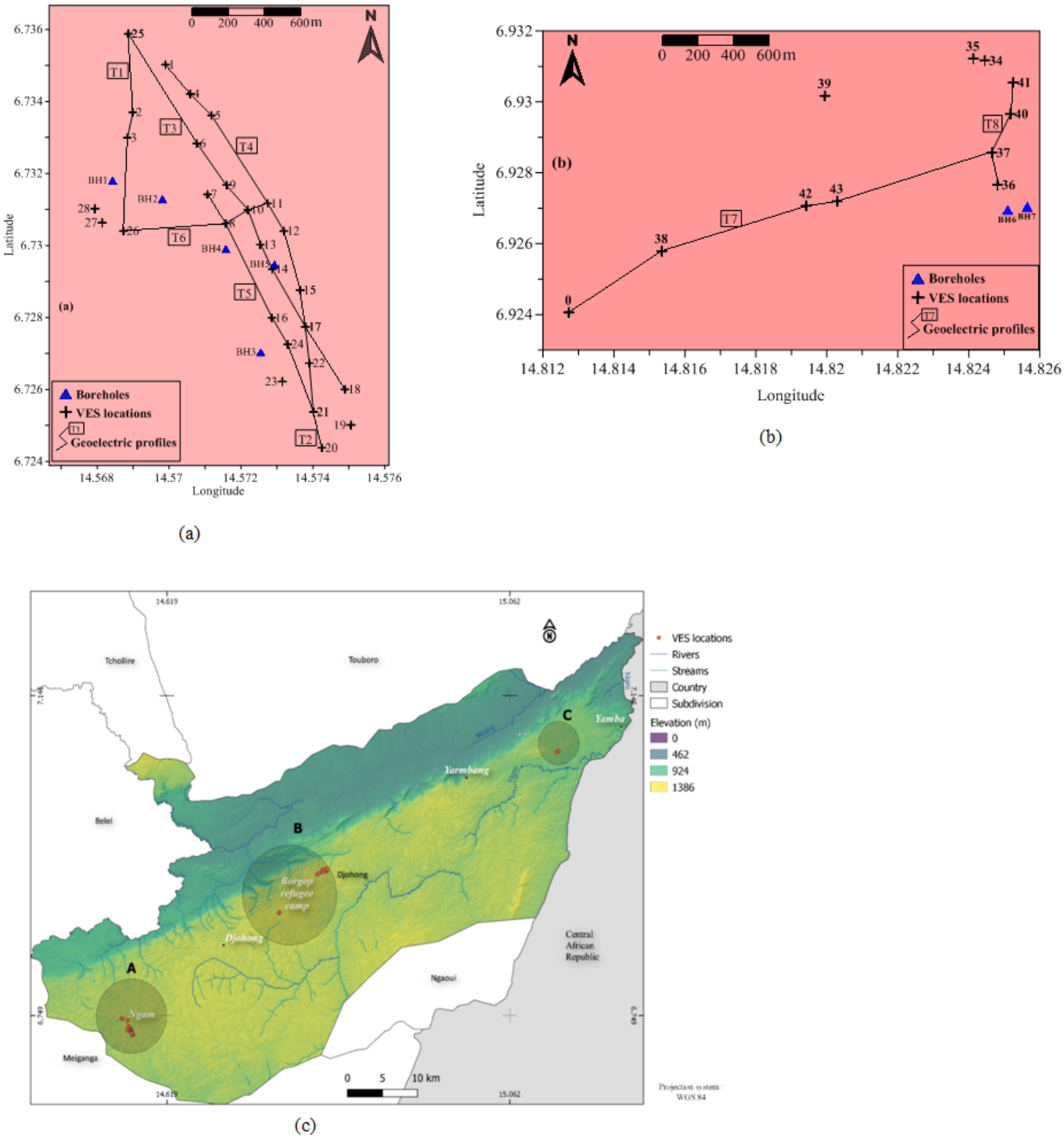

Figure 3

The Location map of both VES stations and the geoelectric profiles of Ngam camp (A) and Borgop camp (B) from the topographic map of Djohong municipality (C).

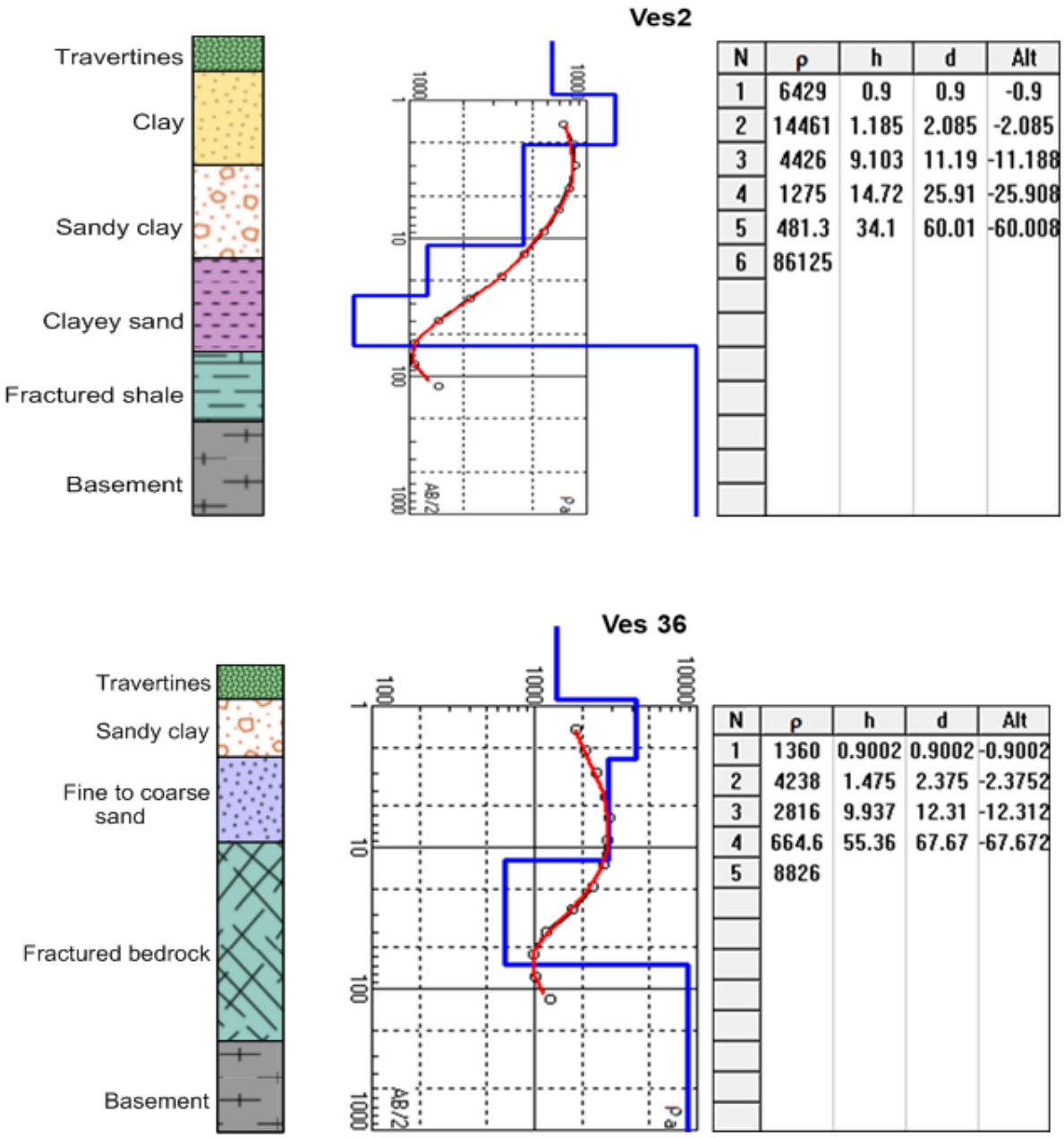

Figure 4

Interpreted VES data at sounding points 2 (Top) and 36 (bottom) correlated with boreholes lithological units (BH5, BH7) in the study area.

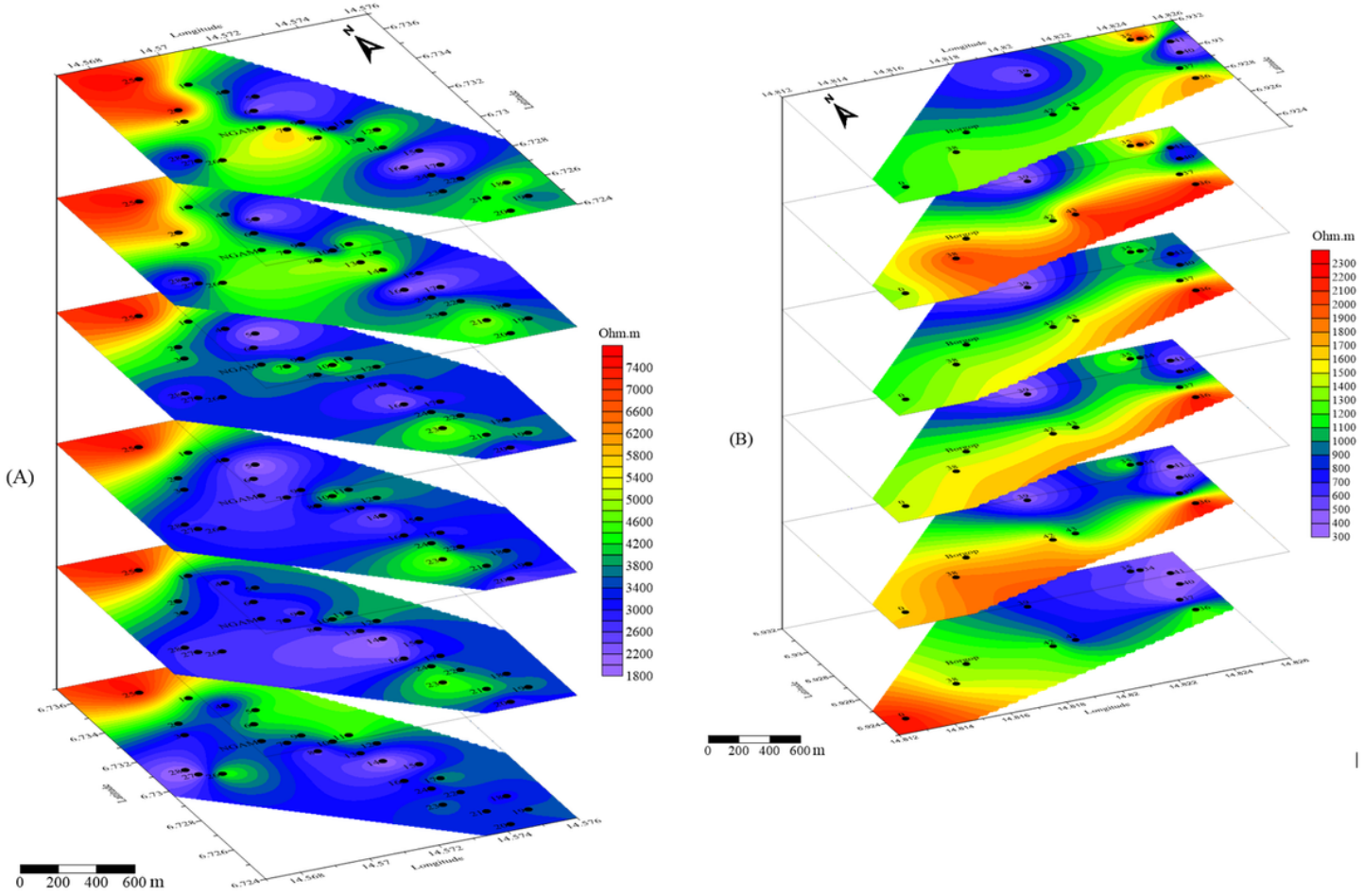

Figure 5

Apparent resistivity slice maps of Ngam camp (A) and Borgop camp (B) for AB spacing of 3, 8.8, 26.4, 38, 55 and 116 m (from top to bottom) respectively.

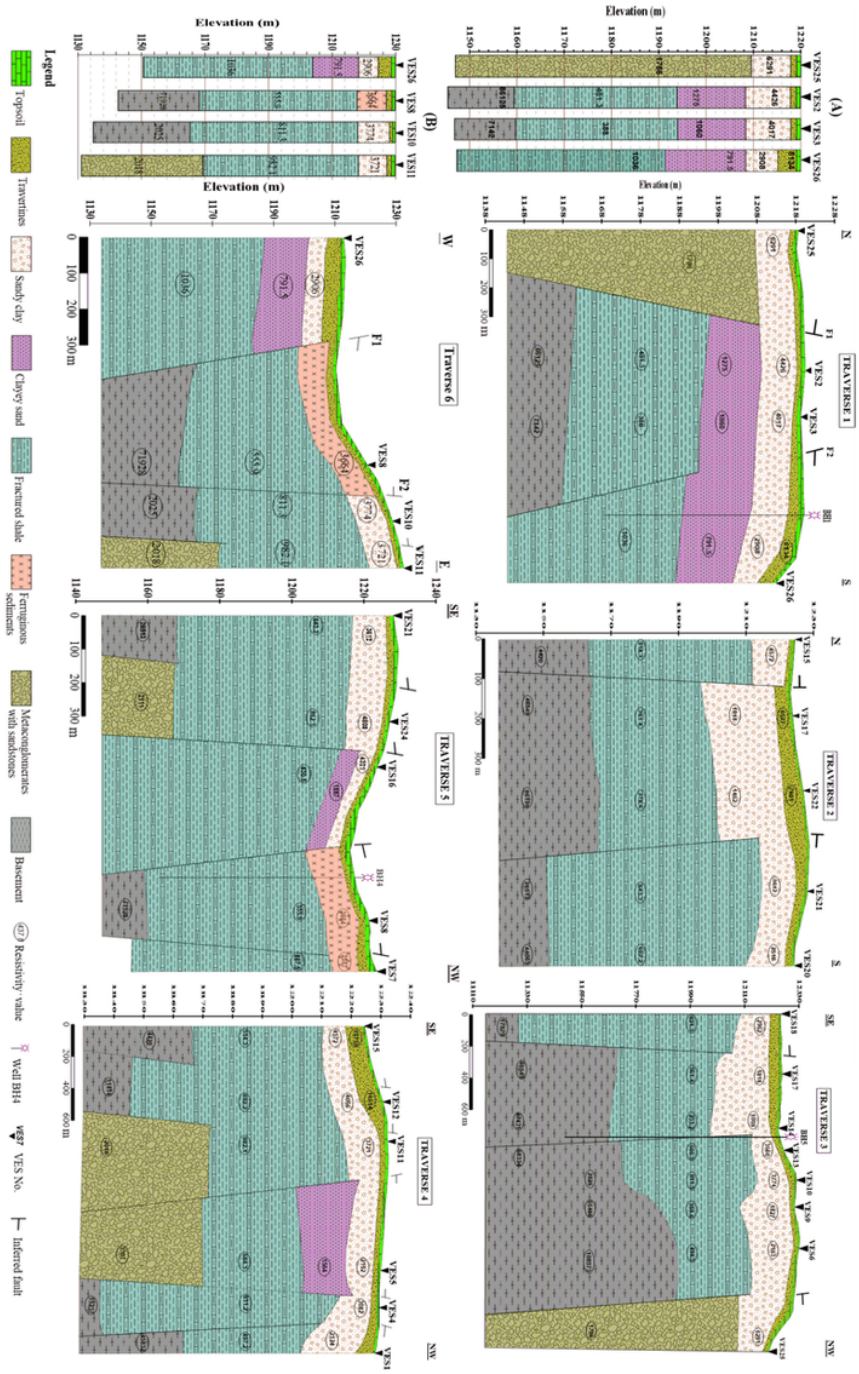

Figure 6

Geoelectric cross-sections of Ngam camp (Traverse 1, 2, 3, 4, 5 and 6) with apparent resistivity of Traverse 1 (A) and Traverse 6 (B).

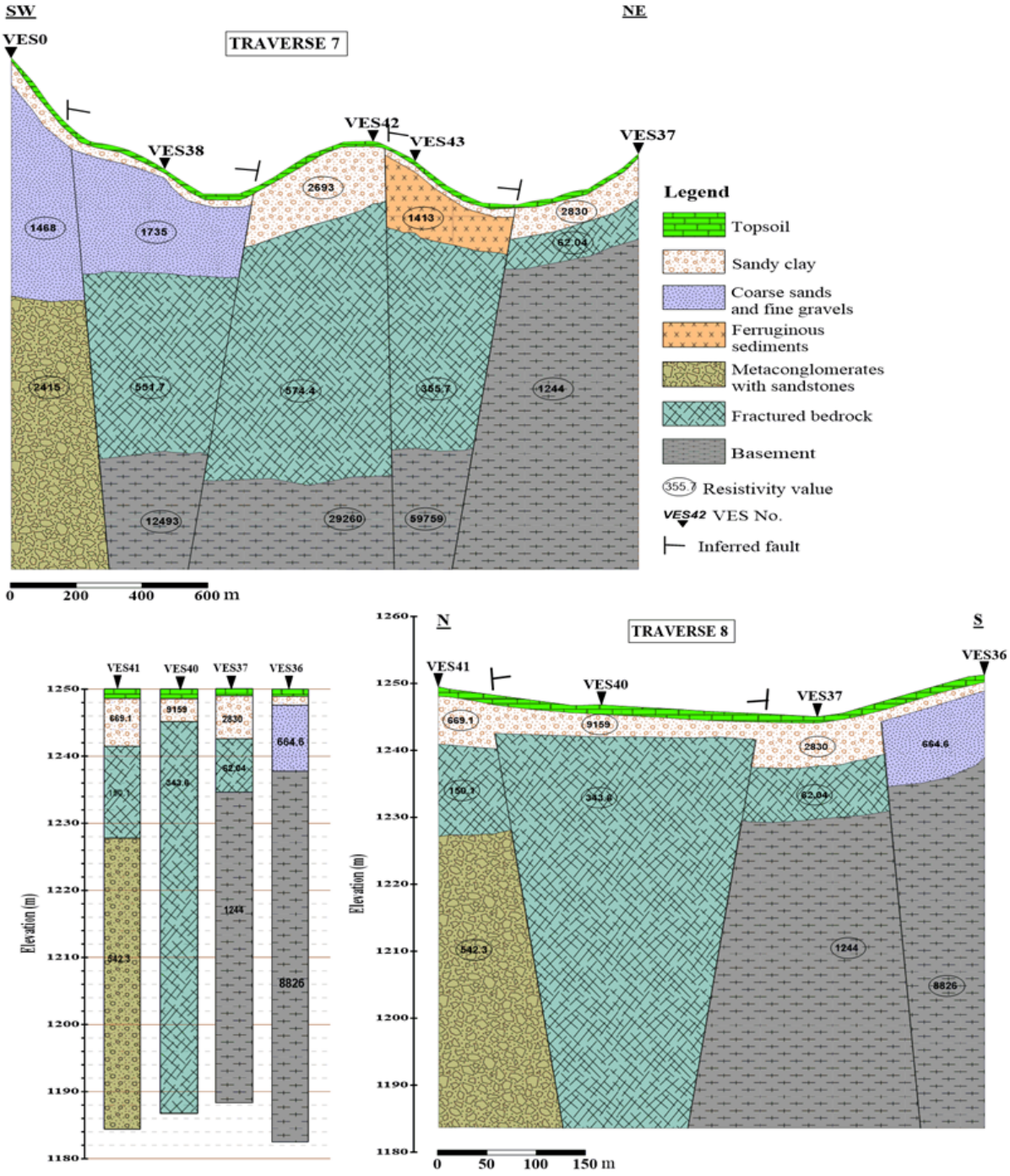

Figure 7

Geoelectric cross-sections of Borgop camp (Traverse 7 and 8) with apparent resistivity of traverse 8.

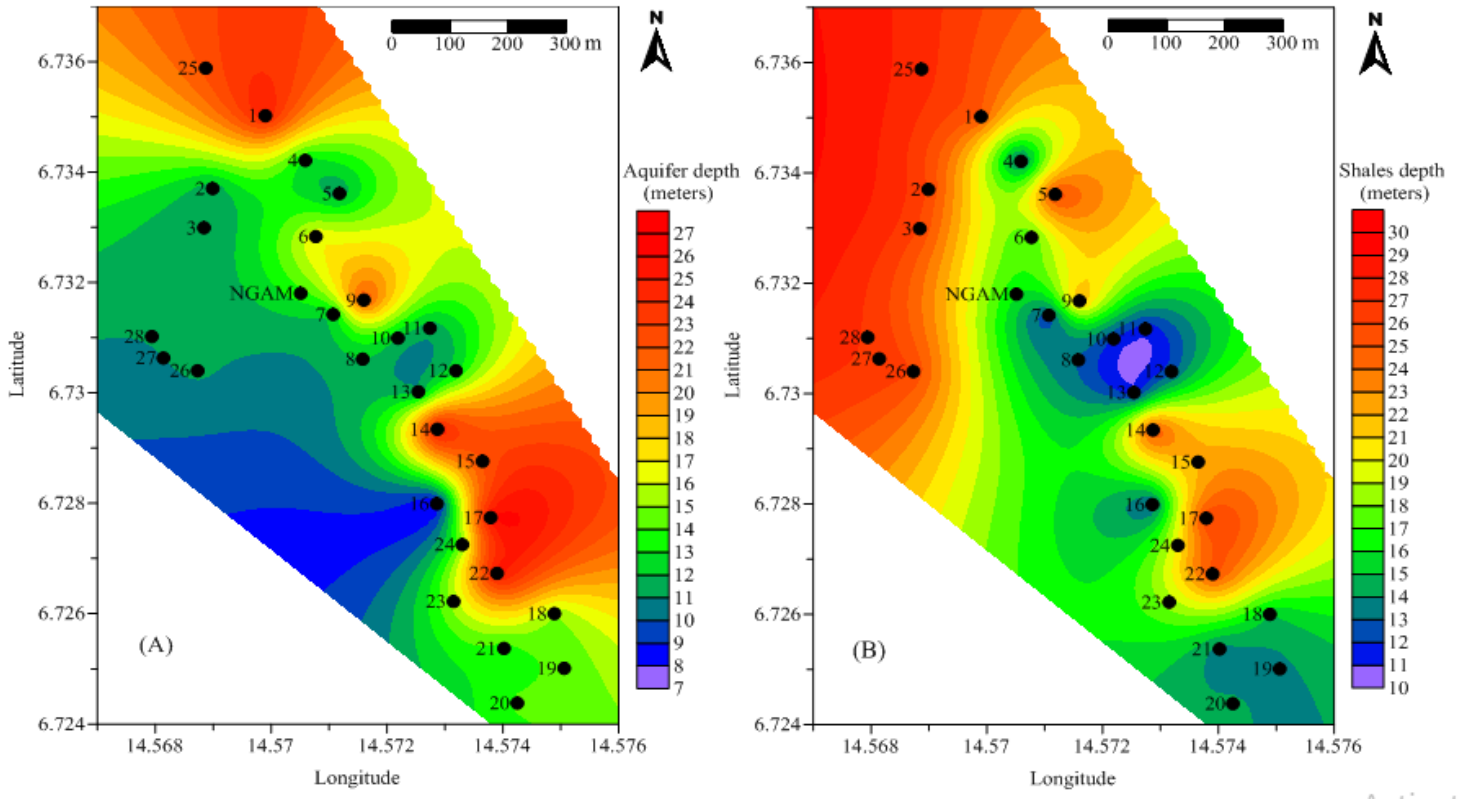

Figure 8

Depth map of the aquifers (upper and lower) (A) and depth map of the lower aquifer (B) in Ngam camp.

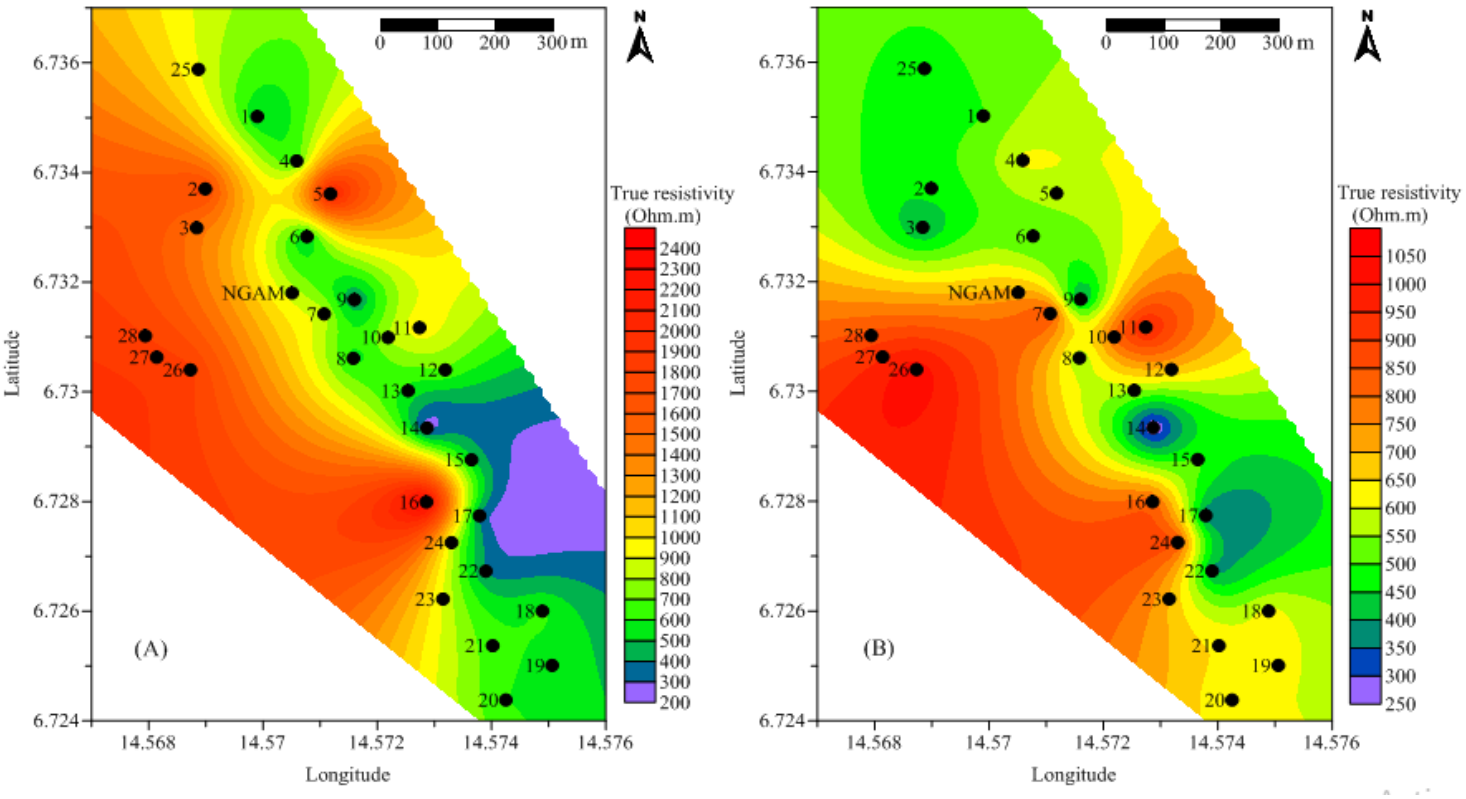

Figure 9

True resistivity map of the aquifers (upper and lower) (A) and true resistivity map of the lower aquifer (B) in Ngam camp.

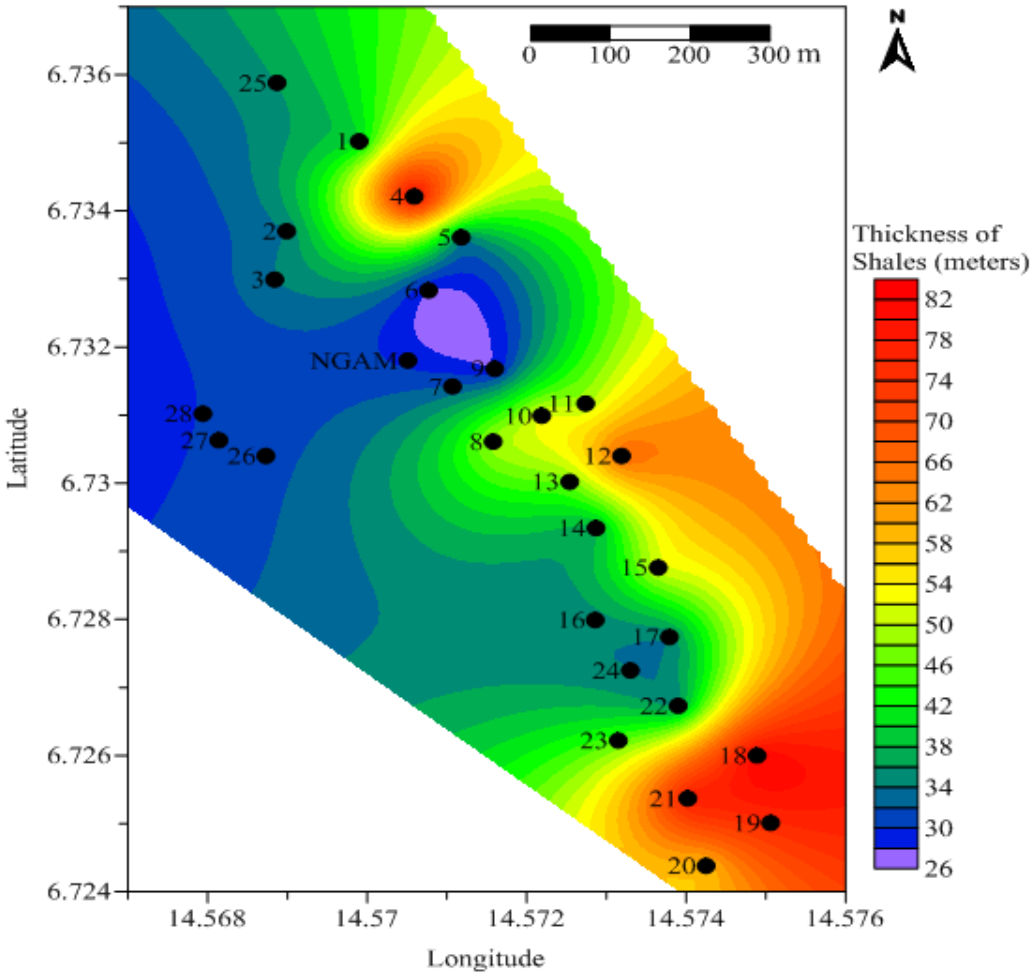

Figure 10

Thickness map of the lower aquifer (fifth geoelectric unit) in Ngam camp.

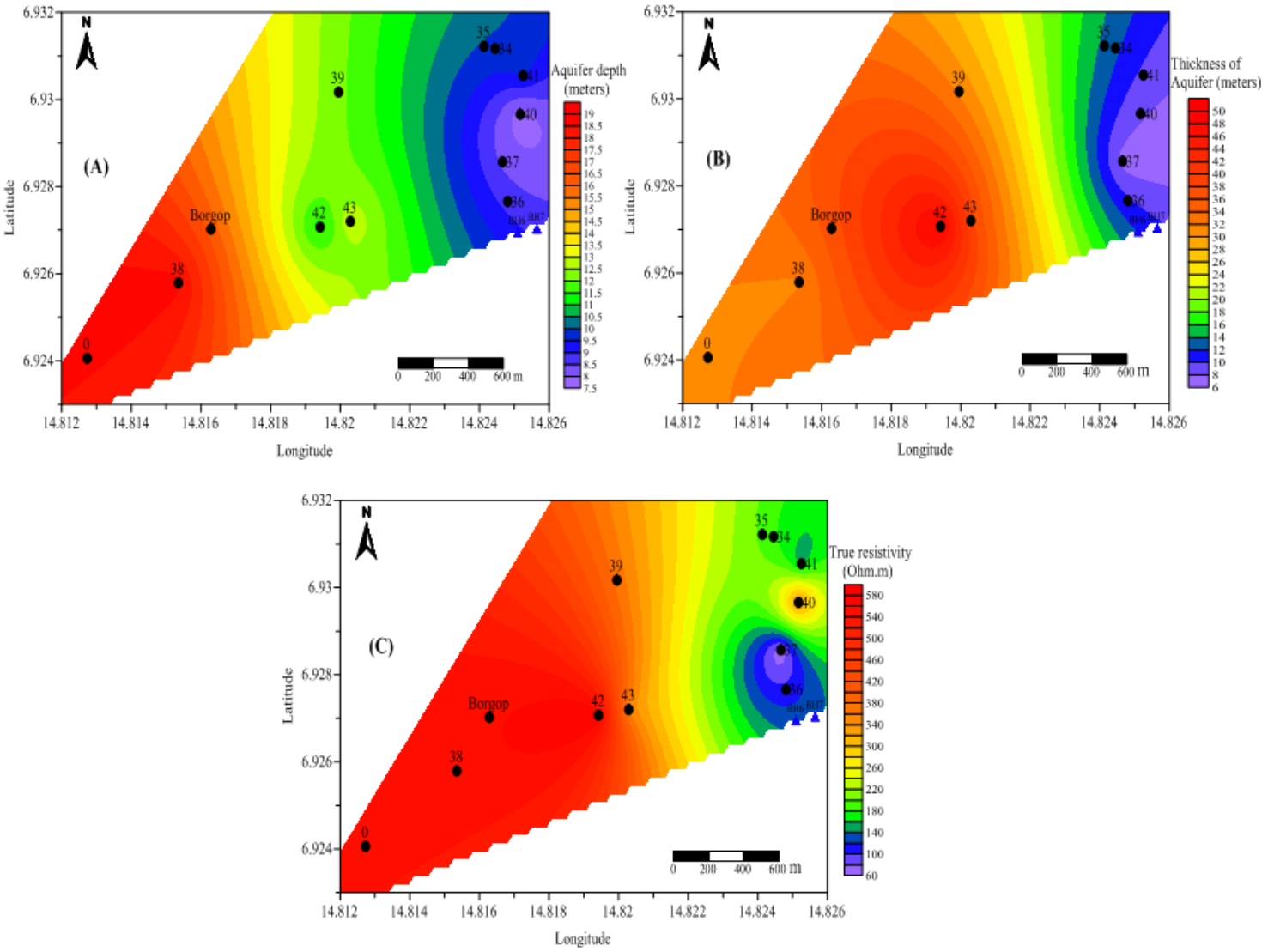

Figure 11

Maps of aquifer of Borgop camp; (A) depth, (B) thickness and (C) true resistivity.